AD-A033 543 INDIANA UNIV BLOOMINGTON DEPT OF CHEMISTRY F/G 7/4
SATURATION OF ENERGY LEVELS IN ANALYTICAL ATOMIC FLUORESCENCE S--ETC(U)
DEC 76 D R OLIVARES, G M HIEFTJE N00014-76-C-0838
UNCLASSIFIED TR-3 NL

1 OF 1
ADA033543

END
DATE FILMED
2 - 77

AD A033543

SECURITY CLASSIFICATION OF THIS PAGE (When Data Entered)

REPORT DOCUMENTATION PAGE

READ INSTRUCTIONS BEFORE COMPLETING FORM

1. REPORT NUMBER: 3	2. GOVT ACCESSION NO.
3. RECIPIENT'S CATALOG NUMBER	
4. TITLE (and Subtitle): SATURATION OF ENERGY LEVELS IN ANALYTICAL ATOMIC FLUORESCENCE SPECTROMETRY. I. THEORY.	5. TYPE OF REPORT & PERIOD COVERED: Interim technical report.
	6. PERFORMING ORG. REPORT NUMBER: 3
7. AUTHOR(s): D.R. Olivares and G.M. Hieftje	8. CONTRACT OR GRANT NUMBER(s): N-14-76-C-0838 / N0014-76-C-0838, NSF-MPS-75-21695
9. PERFORMING ORGANIZATION NAME AND ADDRESS: Department of Chemistry, Indiana University, Bloomington, IN 47401	10. PROGRAM ELEMENT, PROJECT, TASK AREA & WORK UNIT NUMBERS: NR 051-622
11. CONTROLLING OFFICE NAME AND ADDRESS: Office of Naval Research, Washington, D.C.	12. REPORT DATE: December 1976
	13. NUMBER OF PAGES: 50 (12) 53p.
14. MONITORING AGENCY NAME & ADDRESS(if different from Controlling Office)	15. SECURITY CLASS. (of this report): UNCLASSIFIED
	15a. DECLASSIFICATION/DOWNGRADING SCHEDULE

16. DISTRIBUTION STATEMENT (of this Report)

Approved for public release; distribution unlimited

17. DISTRIBUTION STATEMENT (of the abstract entered in Block 20, if different from Report)

18. SUPPLEMENTARY NOTES

Prepared for publication in SPECTROCHIMICA ACTA, PART B

DDC DEC 21 1976 A

19. KEY WORDS (Continue on reverse side if necessary and identify by block number)

saturation spectral power density
theory of saturation
energy-level saturation
atomic fluorescence

20. ABSTRACT (Continue on reverse side if necessary and identify by block number)

The potential importance of energy-level saturation to analytical atomic fluorescence spectrometry has prompted a two-part fundamental investigation into the saturation process. The first part, reported here, develops a model for saturation which is applicable to both resonance and non-resonance fluorescence of atoms in flames or other gaseous media. Provision is made for -considering both collisional excitation and quenching of atoms, and the exciting source can be chosen to be of any desired duration. To illustrate

(over)

DD FORM 1 JAN 73 1473 EDITION OF 1 NOV 65 IS OBSOLETE S/N 0102-014-6601

UNCLASSIFIED

SECURITY CLASSIFICATION OF THIS PAGE (When Data Entered)

176 685

20. the utility of the model, values are predicted for the source spectral power density necessary to saturate several analytically important atomic transitions. Application of the model requires only a knowledge of the kinetic parameters of the energy levels being proved, including Einstein coefficients and quenching rates. Assumptions implicit in the model are discussed and its sphere of valid application considered. Experimental verification of the model will be reported in part II.

OFFICE OF NAVAL RESEARCH

Contract N14-76-C-0838

Task No. NR 051-622

TECHNICAL REPORT NO. 3

SATURATION OF ENERGY LEVELS IN ANALYTICAL ATOMIC FLUORESCENCE SPECTROMETRY
I. THEORY

by

D.R. Olivares and G.M. Hieftje

Prepared for Publication

in

SPECTROCHIMICA ACTA, PART B

Indiana University

Department of Chemistry

Bloomington, Indiana 47401

December, 1976

ABSTRACT

The potential importance of energy-level saturation to analytical atomic fluorescence spectrometry has prompted a two-part fundamental investigation into the saturation process. The first part, reported here, develops a model for saturation which is applicable to both resonance and non-resonance fluorescence of atoms in flames or other gaseous media. Provision is made for considering both collisional excitation and quenching of atoms, and the exciting source can be chosen to be of any desired duration. To illustrate the utility of the model, values are predicted for the source spectral power density necessary to saturate several analytically important atomic transitions. Application of the model requires only a knowledge of the kinetic parameters of the energy levels being probed, including Einstein coefficients and quenching rates. Assumptions implicit in the model are discussed and its sphere of valid application considered. Experimental verification of the model will be reported in part II.

A number of investigators have explored the application of tunable lasers as excitation sources in atomic fluorescence spectrometry (AFS) (1-10). In general, these studies have revealed that laser-excited AFS can provide higher sensitivity, reduced interference from spectral background and radiation scattering, longer linear working curves, greater freedom from quenching effects and source fluctuations, and enhanced multielement capability over AFS excited by conventional sources. Several of these advantages derive directly from the ability of high-power tunable lasers to saturate an atomic transition (6, 11-13).

Energy level saturation occurs in an atomic system when radiationally induced excitation becomes much more rapid than all deactivation processes. Under such conditions, the state from which the excitation transitions originate becomes somewhat depopulated while the excited state population increases. Because the excitation rate producing this depopulation depends upon the photon flux incident on the absorbers, the upper state population can approach that of the lower state, provided that the source irradiance is sufficiently high. When this happens, the atomic system approaches saturation and is said to be bleached.

If an atomic system is bleached or saturated, its absorption is nonlinear and, in fact, approaches zero, since the atoms cannot absorb more energy than is necessary to produce equivalent upper and lower energy level populations. Furthermore, as long as the incident source radiation has a sufficient power density, saturation will be maintained despite the existence of or changes in radiationless depopulation of the excited state. Consequently, the detected spontaneous fluorescence from a saturated atomic system will be constant, since spontaneous radiational deactivation rates depend only on the excited state population. Thus, atomic fluorescence measured under con-

ditions of high source irradiance is immune to source power variations, as long as the power is sufficient to maintain saturation. Also, because the saturated excited state population is governed entirely by radiationally induced processes, quenching of individual excited atoms by environmental (flame) species does not significantly affect the average number of excited atoms, and the detected fluorescence is similarly unaffected. Working curves of sample concentration vs. fluorescence exhibit extended linearity under conditions of energy-level saturation, due to the absence of inner-filter effects (5-7, 10). These effects become unimportant because of the transparency of a "bleached" atomic system to radiation at the exciting wavelength.

Because of the obvious importance of energy-level saturation to laser-excited AFS, it would be useful to know the minimum incident radiant power density which would be necessary to achieve saturation of the energy levels in an atomic system. Such knowledge would enable one to take full advantage of the practical characteristics produced by the saturation effect and would allow a prediction of the feasibility of producing saturation by specially designed conventional (i.e. non-laser) sources.

Previous research work in saturation of atomic energy levels achieved at high spectral irradiance has predicted little, if any, effect of the quenching characteristics of the atom environment on the saturation power density (5, 6, 10-13). Also, all the theoretical models proposed to explain the saturation effect have assumed that steady-state conditions prevail in the radiationally induced excitation process, an assumption which is only valid if the duration of the excitation pulse is much longer than the fluorescence lifetime of the transition being studied. Because typical values of atomic fluorescence lifetimes are 1-20 ns, such steady state conditions do not prevail in atomic systems excited by a short-pulsed, nitrogen-pumped

tunable dye laser (typical pulse width: 5-10 ns), although they are approached when longer duration sources are used. One such source is the flash-lamp-pumped tunable dye laser (typical pulse lengths 1-10 μs).

In the present study, experimental and predicted values of saturation power density were determined and their dependence on atom-environment and on the spectral and spatial characteristics of the irradiance source was ascertained. The study was comprised of and will be reported in two parts. In the part covered here, a theoretical model will be developed for saturation of atomic levels by a radiation pulse of variable duration. The model includes provision for radiationless (collisional) deactivation of excited species and is applicable to complex radiational decay schemes as well as to simpler resonance fluorescence behavior. To illustrate the utility of the model, values of the radiant spectral power density necessary to saturate specific atomic transitions will be calculated and presented, and the dependence of saturation spectral power density on excitation pulse width will be illustrated.

In the second part of the study, to be published later, experimental values of saturation spectral power density will be reported for a number of atomic transitions, using a nitrogen-pumped dye laser as the excitation source (pulse width = 6.5 ns). Conditions necessary for obtaining accurate values of saturation spectral power density will be described and the influence of experimental parameters such as atom environment, atom concentration, and type of transition will be illustrated. Finally, experimental values of saturation spectral power density so obtained will be compared with those predicted by the model developed herein; the resulting agreement, considerably improved over that obtainable using earlier theoretical models, enables useful conclusions to be drawn concerning the feasibility and practicality of employing saturated atomic fluorescence spectrometry for routine analysis.

THEORETICAL ANALYSIS

In this section, a theoretical model is proposed to explain the dependence of the non-steady-state saturation of atomic energy levels on the relative width of the excitation pulse and on the fluorescence lifetime of the observed atomic transition. Also considered theoretically are the influence of quenching species in the atom's environment on the saturation power density and the importance of non-resonance transitions to the saturation process.

Relationship Between Upper-State Population and Fluorescence Yield.

In general, for a spontaneous atomic fluorescence transition from an upper energy level 2 of energy E_2 to a lower energy level 1 of energy E_1, the magnitude of the detected fluorescence radiance (B_F) at a given time (t) is given by

$$B_F(t) = C\, A_{21}\, n_2(t)\, (E_2 - E_1) \qquad (1)$$

where C is a proportionality constant that contains geometrical parameters such as angle of collection of the fluorescent radiation, the length of the absorbing atomic medium, etc.; A_{21} is the Einstein coefficient for the spontaneous transition $2 \rightarrow 1$; $n_2(t)$ is the atom population in the excited energy level 2 at time t; $E_2 - E_1 = h\nu_{21}$ is the energy difference between the levels involved in the transition $2 \rightarrow 1$, where h is the Planck constant and ν_{21} the spectral frequency of the $2 \rightarrow 1$ transition.

From equation 1, the detected fluorescent radiation obtainable from any number of excited atoms is dependent only on the optical design of the radiation-collecting system being used, on fundamental constants which are characteristic of the particular transition being viewed and on the number of atoms that exist in the excited state from which the observed fluorescent transition

originates. Of these parameters, only the excited state population is of significance, the others usually being fixed for any given experimental arrangement.

Because the detected fluorescence is directly proportional to the time-dependent excited-state population [$n_2(t)$], it becomes possible to study the practical significance of energy-level saturation in atomic fluorescence spectrometry merely by examining the effects of saturation on the population of specific upper energy levels involved in the desired fluorescence process. For this reason, all subsequent treatment of saturation processes in this chapter will be oriented toward determining particular excited state populations, with the understanding that such populations can be directly related to fluorescence yields.

Since resonance and direct-line fluorescence (14) are the most frequently used AF transitions in chemical analysis, we will separately consider a two-level and a three-level atomic model, each yielding one of these two kinds of fluorescence transitions. These models will then be used to explain the time behavior of the population of the excited energy level involved in fluorescence as a function of the length of the radiation pulse causing excitation.

Two-Level Model

A diagram of the two energy-level (resonance) atomic model and the mathematical function to describe the time behavior of the exciting radiation pulse are shown in Fig. 1. Fig. 1A illustrates a resonance transition with upper (2) and lower (1) atomic levels of energies E_2 and E_1 respectively, with the relevant activation and deactivation paths of the transition indicated by arrows. In this case, the atomic system is assumed to be irradiated by a beam of photons having a spectral power density $\rho(t)$ which is constant over

the wavelength (frequency) region of interest and which has a time variation described by a square pulse of definable length (Fig. 1B).

In this model, a group of atoms in the lower energy level 1, when exposed to the beam of radiation, moves to the upper energy level 2 by absorption of a quantum each of the incident energy, and at a rate proportional to $B_{12}\rho(t)$. B_{12} is the Einstein coefficient for the stimulated absorption transition $1 \rightarrow 2$. Once in the excited level, the atom can undergo deactivation to the lower energy level either by spontaneous emission, by collision with other species or through emission induced by the incident radiation. The rate constants of these deactivation processes are (respectively):

$A_{21}(sec^{-1})$; the Einstein coefficient for spontaneous emission, which indicates the probability that an excited atom will spontaneously emit, in a random direction, a quantum of energy equal to that of the absorbed radiation ($E_2 - E_1$);

$Z_{21}(sec^{-1})$; the rate of collisional deactivation, or the probability that an excited atom will pass to the lower energy level 1 by collision with other species without emission of radiation;

$B_{21}\rho(t)$ (sec^{-1}); the probability that the excited atom, exposed to the excitation beam of power density, $\rho(t)$, will return to the lower energy level 1 by emission of a quantum in the same direction as the in ident radiation. B_{21} is the Einstein coefficient for the radiationally induced downward transition $2 \rightarrow 1$.

This latter kind of deactivation process is not detected in conventional AFS, even though it is radiational, because of its directional character.

B_{12} and B_{21} are related to A_{21} and each other by

$$A_{21} = \frac{2h\nu_{21}^3}{c^2} B_{21} = \frac{2ch}{\lambda_{21}^3} B_{21} \qquad (2)$$

and

$$B_{21}\, g_2 = B_{12}\, g_1 \tag{3}$$

where h is the Planck constant (6.624×10^{-34} J sec), c the speed of light (3×10^{10} cm/sec), λ_{21} is the wavelength of the $2 \rightarrow 1$ transition and g_1, g_2 are the degeneracies (statistical weights) of energy levels 1 and 2 respectively.

Thus, considering only the activation and deactivation processes mentioned above, and neglecting temperature and pressure broadening of the atomic spectral lines, the rate of population of the excited energy level 2 of this model is given by:

$$\frac{dn_2(t)}{dt} = B_{12}\, \rho(t)\, n_1(t) - (B_{21}\, \rho(t) + A_{21} + Z_{21})\, n_2(t) \tag{4}$$

where $n_1(t)$ and $n_2(t)$ are the time-dependent numbers of atoms in energy levels 1 and 2, respectively.

Assuming that the total number of atoms (N) is distributed among those two levels,

$$N = n_1(t) + n_2(t) \tag{5}$$

By substitution of $n_1(t)$ from Eq. (5) into Eq. (4), the rate of population of the excited level can be found in terms of $n_2(t)$:

$$\frac{dn_2(t)}{dt} = NB_{12}\rho(t) - n_2(t)\, \{a_2 + b_2\rho(t)\} \tag{6}$$

where

$$a_2 = A_{21} + Z_{21} \tag{7}$$

and

$$b_2 = B_{12} + B_{21} \tag{8}$$

It is noteworthy that the constant a_2 is the reciprocal of the fluorescence lifetime (τ') of the observed transition.

In this analysis, the time behavior of the laser pulse [$\rho(t)$] is assumed to be a boxcar function of width t_0 and height ρ_0 (cf. Fig. 1B), mathematically described by

$$\rho(t) = \begin{cases} \rho_0 & 0 \le t \le t_0 \\ 0 & t > t_0 \end{cases} \tag{9}$$

Remembering the shape of this excitation pulse, let us first consider the case in which a steady-state population of the excited level is achieved during the excitation pulse; this situation prevails when the excitation pulse length (t_0) is large compared to the fluorescence lifetime of the transition (τ').

Case I: Steady State Irradiation

Under steady-state irradiation conditions, the change in population of the excited state is negligible so that

$$\frac{dn_2(t)}{dt} \approx 0$$

If the exciting radiation then has a constant power density of ρ_0 (i.e., $t_0 \to \infty$), the steady-state population of energy level 2 [N_2^{ss}], obtained by solving Eq. (6) is given by

$$N_2^{ss} = NB_{12}\left(\frac{\rho_0}{a_2 + b_2\rho_0}\right)$$

or

$$N_2^{ss} = \frac{NB_{12}}{b_2}\left(\frac{\rho_0}{\rho_s + \rho_0}\right) \tag{10}$$

where

$$\rho_s = \frac{a_2}{b_2} \tag{11}$$

Eq. (10) implies that under steady-state conditions, the population of the excited level increases in nonlinear proportion with the peak power density of the excitation pulse (ρ_0), toward a saturation level, [$(N_2)_{sat}$], which can be found from Eq. (10). In Eq. (10), as ρ_0 gets larger and larger, ρ_s becomes less and less significant. Ultimately, the denominator in the parenthetical expression of Eq. (10) becomes approximately equal to ρ_0 and Eq. (10) simplifies to

$$(N_2)_{sat} = \frac{NB_{12}}{b_2} \tag{12}$$

Thus, under steady-state conditions, the saturation population of an atomic system depends only on the fundamental parameters B_{12} and $b_2 = B_{12} + B_{21}$ [Eq. (8)]. From Eq. (3), the values of B_{12} and B_{21} are seen to be related by their statistical weights. Using this information and Eq. (12), the maximum fraction of excited atoms

$$\frac{(N_2)_{sat}}{N} = \frac{1}{(1 + g_1/g_2)} \tag{13}$$

is only dependent on the degeneracies of the levels involved.

In practical work, it has been found useful to define a saturation power density (7) which occurs when $\rho_0 = \rho_s$. In this situation, Eq. (10) becomes

$$(N_2^{ss})_s = \frac{NB_{12}}{b_2} \left(\tfrac{1}{2}\right)$$

or

$$(N_2^{ss})_s = \tfrac{1}{2} (N_2)_{sat}$$

In other words, when the incident power density ρ_0 reaches the value ρ_s, the excited-state population will be 50 percent of that achievable under complete saturation.

Case II. Non-Steady State (Transient) Irradiation

When the duration (t_0) of the radiation pulse producing excitation is comparable to or shorter than the fluorescence lifetime of the upper state of the transition being observed, the steady-state assumption made in the previous section does not hold, and the change in population of the excited level $[dn_2(t)/dt]$ cannot be neglected. In this non-steady-state situation, the populations of the excited level both during ($0 \leq t \leq t_0$) and after ($t > t_0$) termination of the excitation pulse can be obtained by solving Eq. (6), and are given by:

i) for $0 \leq t \leq t_0$

$$n_2(t) = NB_{12}\rho_0 \frac{\{1 - e^{-(a_2 + b_2\rho_0)t}\}}{(a_2 + b_2\rho_0)} \qquad (14)$$

and

ii) for $t > t_0$

$$n_2(t) = \frac{NB_{12}\rho_0}{a_2} (e^{a_2 t_0} - 1)\, e^{-a_2 t} \qquad (15)$$

A plot of the above expressions reveals the time behavior of the excited state population expected when exciting radiation pulses of any length are employed. For convenience, Eqs. (14) and (15) will be plotted as the fraction of excited atoms $\frac{n_2(t)}{N}$, rather than directly as upper-level populations. As an example, Fig. 2 shows the changing fractional upper-level population expected under conditions prevailing during excitation by a nitrogen-pumped tunable dye laser. To construct this plot, an excitation pulse of 5 ns duration was assumed; this value is typical of pulse lengths in nitrogen-pumped tunable dye lasers. For the a_2, $b_2\rho_0$ and B_{12} parameters, values typical of many atomic fluorescence transitions were used, specifically:

$$a_2 = 10^9 \text{ Sec}^{-1}$$

$$b_2\rho_0 = a_2$$

$$B_{12} = b_2/2 \qquad (g_1 = g_2 \text{ in Eqs. (3) and (8))}$$

In Fig. 2, the fraction of excited atoms rises as long as the exciting radiation is applied; the rise time of the population increase is calculated to be 0.5 ns, which corresponds to the quantity $(a_2 + b_2\rho_0)^{-1}$, as one would expect from Eq. (14). After termination of the excitation pulse, the population of the excited level decays with a time constant of 1 ns, which corresponds to the effective fluorescence lifetime of the atomic transition in a flame environment [$\tau' = a_2^{-1}$, cf. Eq. (15)]. In this special case, the half-width of the curve describing the fraction of excited atoms is equal to 5 ns, the

same as the length of the excitation pulse.

As mentioned earlier, the variation in excited-state population illustrated in Fig. 2 can be experimentally followed by monitoring the spontaneous fluorescence emitted during depopulation of the excited state. Because the magnitude of spontaneous fluorescence is directly proportional to the excited-state population [cf. Eq. (1)], a plot of measured fluorescence vs. time should generate a curve such as Fig. 2 directly. However, because of limitations in instrumentation, it is often more convenient to measure the <u>average</u> fluorescence which is produced over a specified time interval. In the specific but frequently encountered example of gated detector (boxcar integrator) being employed, the recorded signal will be the time average of the fluorescence radiation, detected over the sampling gatewidth of the gated detector. For convenience, let us assume a sampling gatewidth equal to the laser pulse duration (t_0). The average population of the excited energy level (N_2) during the excitation pulse (which determines the magnitude of the detected fluorescence signal) can then be calculated:

$$N_2 = \overline{n_2(t)} = \frac{1}{t_0} \int_0^{t_0} n_2(t)dt \tag{16}$$

By substitution of Eq. (14) into Eq. (16) and integration, one obtains

$$N_2 = NB_{12} \left(\frac{\rho_0}{a_2 + b_2\rho_0} \right) \{1 - D\} \tag{17}$$

where

$$D = \frac{\left(1 - e^{-(a_2+b_2\rho_0)t_0}\right)}{(a_2+b_2\rho_0)t_0} \tag{18}$$

As in the case of steady-state population of the excited state, a value for the radiant power density can be defined (ρ_s^{NSS}) which is necessary to produce an upper state population just half of that required for saturation. Thus,

by solving Eq. (17) for $\rho_0 = \rho_s^{NSS}$ and doing a series expansion of the exponential term in the expression for D, one obtains the following expression for ρ_s^{NSS}

$$\rho_s^{NSS} \simeq (b_2 t_0)^{-1} \tag{19}$$

which implies that under non-steady-state population of the excited level, the saturation spectral power density depends only on the Einstein coefficients for induced transitions (B_{12}, B_{21}) and on the duration of the excitation pulse but is independent of the rate of quenching collisions. A comparison of Eqs. (10) and (17) reveals that under non-steady-state conditions, the rate-controlled average population of the excited level (N_2) differs from the steady-state population (N_2^{SS}) by an amount given by the D term (cf. Eq. 18).

According to Eq. (18), the departure (D) of N_2 from N_2^{SS} is determined, at any given value of ρ_0, by the relative magnitudes of the excitation pulse length (t_0) and the excitation time constant given by $(a_2 + b_2\rho_0)^{-1}$. For values of t_0 much larger than $(a + b\rho_0)^{-1}$, D becomes negligible, and N_2 becomes equal to N_2^{SS}, an altogether expected result. In contrast, at values of t_0 comparable to or smaller than $(a_2 + b_2\rho_0)^{-1}$, the population of the excited level (N_2) rises with increasing ρ_0 toward the saturation level at a rate determined primarily by the term D and, therefore, by the t_0, a and b parameters.

The rate-controlled population process described above is illustrated in Fig. 3, for excitation pulses of several different lengths. In Fig. 3, the fraction of excited atoms (N_2/N) has been calculated from Eq. (17) and is plotted as a function of the excitation power density ρ_0 (watts/cm^2 Hz), for excitation pulses of 1 ns, 10 ns and 1 μs duration. These particular

plots correspond to the behavior predicted for the $S_0 \rightarrow P_1$ transition of Ba (553.5 nm). For this transition, a fluorescence lifetime (τ) of 8.5 ns has been measured (15) in the absence of foreign quenching gases (i.e., when $Z_{21} \approx 0$). For the plots in Fig. 3, the a_2 and b_2 parameters were calculated by assuming that the rate of collisional deactivation would, in a flame environment, be approximately ten times faster than the rate of deactivation by spontaneous emission (i.e., $Z_{21} \approx 10\ A_{21}$) and by using the relationship between the A_{21} and B_{21} coefficients given in Eqs. (2) and (3).

From Fig. 3, the population of the excited level rises toward the saturation level faster when a 1 μsec pulse is used (curve A) than when a 1 nsec excitation pulse is employed (curve C). These results are entirely expected; when the excitation pulse (t_0) is much longer (1 μsec) than the fluorescence lifetime of the transition and therefore also much longer than $(a_2 + b_2\rho_0)^{-1}$, steady-state-population of the excited level should prevail. In contrast, a 1 ns duration excitation pulse requires non-steady-state (kinetically controlled) population of the excited level, because the length of the pulse is smaller than the fluorescence lifetime of the transition and comparable to $(a_2 + b_2\rho_0)^{-1}$ for low values of ρ_0. When a 10 ns excitation pulse is assumed (curve B), the duration of the pulse is comparable to the fluorescence lifetime, but longer than $(a_2 + b_2\rho_0)^{-1}$. Therefore, the fraction of excited atoms varies with exciting power density just as in curve A, but with a lower magnitude; this behavior arises because the D factor (cf. Eq. (18)) is not negligible in this case.

A comparison of curves A and C in Fig. 3 reveals that the extent of departure of each curve from the behavior expected for steady-state population decreases as the spectral power density ρ_0 increases. In fact, at very high values of ρ_0, the fraction of excited atoms should become the same in all cases.

In order to calculate the saturation power density corresponding to each of the curves in Fig. 3, we must know the maximum fraction of excited atoms which would exist during complete saturation of the atomic system. In the case of the $S_0 \rightarrow P_1$ transition of Ba under consideration, a maximum fraction of excited atoms equal to 0.75 was calculated from Eq. (13), with $g_1 = 1$ and $g_2 = 3$. From Fig. 3, the saturation power density (i.e., the spectral power density necessary to produce a fraction of excited atoms equal to 0.375) varies with the duration of the excitation pulse.

Table I shows calculated values of saturation power densities for the excitation pulses considered in Fig. 3. From Table I, a 1 ns exciting pulse must be over twice the power density of a 1 μs pulse to produce an upper level population equal to 50 percent of that prevailing at total saturation. This result is a consequence of the kinetically controlled nature of the saturation process which must be dominant when short exciting pulses are used.

Considerations on Predicted Saturation Power Densities

From Eq. (17), the dependence of the excited-state population on the excitation power density is determined by the magnitude of the a_2 and b_2 lumped parameters for a given excitation pulse duration. Therefore, the saturation power density which is predicted by the described model is determined by both fundamental atomic parameters and environmental factors, such as the fluorescence lifetime of the transition and the rate of collisional deactivation produced by the atom environment (cf. Eqs. (7) and (8)). Unfortunately, accurate values for collisional deactivation rates in a flame environment are not often available; furthermore, the fluorescence lifetimes listed for most atomic transitions contain significant uncertainties. To better appreciate the utility of this theoretical approach, let us then

consider the effect of the accuracy of these parameters on the predicted saturation curves and on the calculated saturation power densities. In the following considerations, the same transition of Ba which was described earlier in this section will be employed.

First, let us assess the importance of uncertainties in the rates of collisional relaxation (Z_{21}). In a flame or other atomizer environment, the fluorescence lifetime of any given atomic transition will be shortened by collisions between excited atoms and other flame species. Such behavior was verified experimentally in this laboratory by measurement of fluorescence lifetimes of atomic transitions in the flame environment and comparing those values to lifetimes of isolated atoms.

The effect of the rate of collisional deactivation upon theoretical saturation curves is shown in Figs. 4 and 5 for excitation pulse lengths of 1 μs and 6.5 ns respectively. In constructing Fig. 5, we have assumed a 6.5 ns pulse length because it corresponds to the excitation pulse of a nitrogen-laser-pumped tunable dye laser which was employed in the experimental measurements of saturation power densities to be described in a later communication. In both Figs. 4 and 5, curve A corresponds to the saturation curve where the atom environment is free of foreign quenching species ($Z_{21} \approx 0$), while curves B and C correspond to atom environments where the rate of collisional deactivation is assumed to be 5 and 10 times faster than the rate of spontaneous emission ($Z_{21} = 5A_{21}$, $10A_{21}$), respectively.

When a 1 μs excitation pulse is used to excite an atomic medium relatively free of quenching species (Fig. 4A), saturation of the excited level is achieved at relatively low values of incident spectral power density. However, in the presence of quenching species (Figs. 4B and 4C), the fraction of excited atoms rises toward the saturation level at a rate which is in-

versely proportional to the rate of collisional deactivation.

If a 6.5 ns excitation pulse is employed (cf. Fig. 5), the saturation curve is affected much in the same way by collisional de-excitation as when the longer (1 μs) pulse is used. However, because the excited state population is determined mainly by radiationally induced transitions when the 6.5 ns pulse is applied, saturation is achieved only at higher spectral power densities than for the 1 μs pulse, where a steady-state population of the excited level prevails. A comparison of curves A, B, and C in either Figs. 4 or 5 reveals that the atomic system approaches saturation as the spectral power density increases regardless of the occurrence of quenching collisions. In fact, at spectral power densities much higher than the saturation power density (ρ_S), the fraction of excited atoms becomes essentially independent of the rate of collisional deactivation. This behavior is expected because at high power densities, radiationally induced transitions ($b_2\rho_0$) become dominant in the population and depopulation of the excited energy level.

The calculated saturation spectral power densities corresponding to the different curves in Figs. 4 and 5 are given in Table II. In this table, ε is the fractional (expressed as a percentage) difference between the saturation power densities which were calculated for the 6.5 ns and 1 μsec excitation pulse lengths (columns 2 and 3 of Table II). From a practical standpoint, ε expresses the relative error which would exist in the calculated value of saturation power density if steady-state conditions had been assumed, but a 6.5 ns excitation pulse were employed.

Several interesting and important observations can be made from Table II. When a 1 μs excitation pulse is assumed, there is a one order of magnitude difference between the values of ρ_S calculated for an atomic medium

relatively free of quenching species ($Z_{21}/A_{21} \approx 0$) and that pertaining to a medium where the rate of collisions is one order of magnitude greater than the rate of spontaneous emission ($Z_{21}/A_{21} = 10$). In comparison, the dependence of ρ_s on quenching is smaller when a 6.5 ns excitation pulse is assumed, although the values of ρ_s are higher than those required for the 1 μs pulse. Also, Table II indicates that the error produced by assuming a steady-state population of the excited level, in the case of a 6.5 ns pulse, decreases as the quenching factor (Z_{21}/A_{21}) increases. This behavior arises because, as collisional deactivation (Z_{21}) increases, the effective fluorescence decay rate of the atomic transition (a_2) becomes comparable to or smaller than the duration of the excitation pulse. Consequently, the 6.5 ns pulse begins to appear more and more like a continuous (in time) radiation level, so that steady-state irradiance conditions are approached.

Another parameter which might cause significant error in the calculated values of saturation power density is the fluorescence lifetime of the transition being considered. The uncertainties in published lifetimes are substantial, and the value finally used in the calculation directly determines the rate of depopulation of the excited energy level, thereby strongly affecting the incident power density required to produce saturation. A plot of saturation curves obtained from Eq. (17), assuming values of 4, 8 and 16 ns for the fluorescence lifetime of the Ba transition considered and a 6.5 ns pulse duration are shown in curves A, B and C of Fig. 6. As expected, the fraction of excited atoms is greatly dependent upon the assumed value of the fluorescence lifetime. Predicted values of saturation power density corresponding to the curves in Fig. 6 are shown in Table III. In this table, the values of ρ_s increase as τ becomes larger than the duration of the excitation pulse. This table also shows the error (ε) in the predicted saturation power density which would be caused by assuming values of the fluorescence

lifetime that are 50 percent smaller or higher than the "real" fluorescence lifetime (8 ns) of the studied transition.

The foregoing considerations reveal that an accurate knowledge of the fluorescence lifetime of the transition and of the rate of collisions is necessary in order to predict accurate saturation power densities of an atomic system irradiated with a pulse of a given duration. Using the two-energy-level model described earlier, predicted values of the saturation power density for several elements are shown in Table IV. In the table is also listed the wavelength of the particular transition for each element being considered, and the values of the fluorescence lifetime available in the literature. In calculating these saturation power densities, we have assumed the rate of collisions to be ten times that of spontaneous emission ($Z_{21} \approx 10A_{21}$) and an excitation pulse of 6.5 ns duration.

The effect of the assumed fluorescence lifetime on the saturation power density of the excited level becomes particularly strong in the case of Cd which has a relatively long fluorescence lifetime (35 ns). Table IV also shows that a higher spectral power density is required to saturate atomic levels in the ultraviolet region (e.g., Mg) compared to atomic levels in the visible spectral region (e.g., Ca, In, Sr, etc.). This behavior is consistent with the dependence of the Einstein A coefficient for spontaneous emission on the cube of the frequency of the transition being studied.

Spectral Irradiance Considerations

It is both worthwhile and instructive to consider the limits of the equations describing steady-state and non-steady-state population of an excited level [Eqs. (10) and (17)] under conditions of extremely low or high spectral irradiance. These special cases will be examined separately.

Limits Occurring During Steady-State Excitation

For spectral power densities (ρ_0) much less than the saturation power density ($\rho_0 << \rho_s$), the population of the excited level becomes, from Eq. (10):

$$N_2^{ss} \approx \frac{NB_{12}}{a_2} \rho_0 \tag{20}$$

Eq. (20) predicts that under steady-state illumination at low spectral power densities, the population of an excited level will be linearly proportional to the effective fluorescence lifetime of the transition ($\tau' = a_2^{-1}$) and will also increase in linear proportion with the power density (ρ_0) of the excitation source. This is just the behavior observed in conventional-source atomic fluorescence.

At excitation source densities much higher than the saturation power density (ρ_s) the population of the excited level will become independent of the spectral radiance of the source and of the fluorescence lifetime of the transition as given by Eqs. (12) and (13). This behavior has been observed by other workers (6).

Limits Occurring During Non-Steady-State Excitation

At low spectral irradiances, the probability of induced transitions ($b_2\rho_0$) becomes negligible compared to the probabilities of collisional deactivation and spontaneous emission (namely, $b_2\rho_0 << a_2$). Therefore, at low incident spectral power densities, non-steady state population of an excited level, given by Eq. (17), becomes

$$N_2 \approx \frac{NB_{12}\rho_0}{a_2} \left\{ 1 - \frac{(1-e^{-a_2 t_0})}{a_2 t_0} \right\} \tag{21}$$

From Eq. (21) we see that N_2 (and thus any detected spontaneous fluorescence) increases in linear proportion with ρ_0, but its magnitude depends on

the relative length of the excitation pulse t_0 and the effective fluorescence lifetime of the transition τ' ($\tau' \approx a_2^{-1}$). In the case of a source of low spectral radiance and pulse duration much longer than τ' (conventional excitation source), the population of the excited level (Eq. (21)) becomes equal to the steady-state population at low spectral irradiances given by Eq. (20), as one would expect.

At high spectral irradiances, the probability of radiationally induced transitions ($b_2\rho_0$) becomes larger than the probabilities of spontaneous and collisional deactivation (a_2). Under these conditions, Eq. (17) reduces to the following relation

$$N_2 \approx N \frac{B_{12}}{b_2} \left\{ 1 - \frac{(1 - e^{-b_2 \rho_0 t_0})}{b_2 \rho_0 t_0} \right\} \tag{22}$$

indicating that the population of the excited level becomes independent of the effective fluorescence lifetime τ' and varies in nonlinear proportion with both the rate of radiationally induced transitions and the duration of the excitation pulse.

From Eq. (22), for an excitation pulse of longer duration than $(b_2\rho_0)^{-1}$ or for a pulse of amplitude (ρ_0) greater than $(b_2 t_0)^{-1}$, the population of the excited state becomes:

$$N_2 \approx N \frac{B_{12}}{b_2} = \frac{N}{(1 + g_1/g_2)} \tag{23}$$

which is the same as the maximum population of the excited level under steady-state saturation conditions [Eqs. (12) and (13)]. Eq. (23) implies that at high power densities ($\rho_0 >> \rho_s$) or under steady-state conditions ($t_0 >> (b_2\rho_0)^{-1}$), the atomic medium becomes transparent to the exciting radiation and the population of the excited level is only dependent on the degeneracies of the energy levels involved in the transition and on the atomic population free to absorb the incident radiation.

Three-Level Model

Because of the high available peak power of tunable dye lasers, non-resonance transitions, particularly direct-line fluorescence and step-wise fluorescence, have become potentially useful for trace analysis. Therefore, it is important to consider the behavior and practical applications of such transitions under conditions of near saturation of the relevent atomic energy levels. For this purpose, we will consider the three-energy-level model illustrated in Fig. 7A. As with the two-state model, it will be assumed that a number (N) of three-state atoms is illuminated by an excitation pulse resembling a boxcar function of duration t_0 and peak spectral power density ρ_0. Such a pulse is portrayed in Fig. 7B. As before, the exciting radiation will be assumed to be constant in magnitude over the atomic absorption bandwidth.

The activation and deactivation pathways in the three-level atom, shown by arrows in Fig. 7A, correspond to the following.

Population of Level 2. Excitation of an atom from energy level 1 to energy level 2 can occur by absorption of a quantum of incident radiation. The rate of this process is given by $B_{12}\,\rho(t)$, where B_{12} is the Einstein coefficient for the radiationally induced transition $1 \rightarrow 2$, as defined earlier. Also, an atom in energy level 3 can be excited to level 2 by collision with flame species or through other thermal processes. The rate of this excitation event is given by Z_{32} and becomes important only in cases where the energy separation between energy levels 2 and 3 is comparable to or smaller than the thermal energy of the flame (i.e., $E_2 - E_3 \lesssim kT$).

An atom originally in level 1 can also be thermally or collisionally excited to level 2. However, the energy difference between these states will be larger than that between levels 2 and 3, so that such collisional

excitation is less probable. In the present case, non-radiational excitation from level 1 to level 3 will be neglected.

Depopulation of Level 2. Once in excited level 2, the atom can relax through the following paths:

i) by radiational deactivation to level 1, involving spontaneous emission (in a random direction) of a quantum of energy equal to that in the incident radiation. This process is called resonance fluorescence and its rate or probability is given by the Einstein coefficient for spontaneous emission A_{21}.

ii) radiational deactivation to level 3, by spontaneous emission (again in a random direction), of a quantum of energy, $(E_2 - E_3)$, different from that of the incident radiation. The rate of this process, termed non-resonance direct-line fluorescence, is given by the Einstein coefficient for spontaneous emission A_{23}.

iii) radiationless deactivation to either level 1 or level 3 through collisions with foreign species in the flame. The rates of these collisionally induced transitions are given by Z_{21} and Z_{23}, respectively.

iv) radiationally induced deactivation to level 1 with emission of a quantum of the same energy and in the same direction as the incident radiation. The rate of this process is given by $B_{21}\,\rho(t)$, where B_{21} is the Einstein coefficient for the induced transition $2 \rightarrow 1$.

Population and Depopulation of Level 3. Atoms in energy level 3 will relax to energy level 1 by spontaneous emission at a rate given by A_{31} and by collisions with flame species at a rate given by Z_{31}. Excitation of atoms from level 1 to level 3 is produced by collision of atoms in level 1 with flame species and has a rate Z_{13}; collisional excitation from level 3 to level 2 can also occur and will have a rate Z_{32}.

In accordance with these activation and deactivation pathways, the rate of population of energy levels 2 and 3 can be shown to be:

$$\frac{dn_2(t)}{dt} = n_1 B_{12}\rho(t) - n_2\left[B_{21}\rho(t) + a_{23} + a_{21}\right] + n_3 Z_{32} \tag{24}$$

and

$$\frac{dn_3(t)}{dt} = n_2 a_{23} + n_1 Z_{13} - n_3(a_{31} + Z_{32}) \tag{25}$$

where

$$a_{21} = A_{21} + Z_{21}, \tag{26}$$

$$a_{23} = A_{23} + Z_{23}, \tag{27}$$

$$a_{31} = A_{31} + Z_{31} \tag{28}$$

and n_1, n_2 and n_3 are the time-dependent atom populations of energy levels 1, 2 and 3, respectively. In this and the following treatment, the simplified notation n_i will be used rather than $n_i(t)$. The reader should recall the time-dependent nature of these parameters, however.

Assuming that the total atom population (N) is entirely distributed among the three energy levels considered,

$$N = n_1 + n_2 + n_3 \tag{29}$$

In the case of direct-line fluorescence, the signal detected is the fluorescence radiation produced by the spontaneous transition from level 2 to level 3. Therefore, the pertinent energy level in determining saturation will be upper level 2. By contrast, during stepwise fluorescence, the signal detected is the radiation produced by the spontaneous transition from level 3 to level 1; consequently, the population of energy level 3 will determine the approach to saturation. Further discussions of saturation of this three-level atom need therefore concern only the populations of level 2 or level 3, depending on whether direct-line or stepwise fluorescence is being considered.

The probability of observing either direct-line or stepwise fluorescence, or of populating any given energy level depicted in Fig. 7, depends largely on the rates of populating or depopulating level 3. To see why this is so, let us consider the cases of direct-line fluorescence and stepwise fluorescence separately.

Direct Line Fluorescence

Because direct-line fluorescence ordinarily involves the observation of transitions corresponding to frequencies in the ultraviolet-visible spectral region, the spacing between energy levels 2 and 3 must be quite large, and will generally be much greater than the thermal energy (kT) available in the flame. Consequently, collisionally induced transitions from level 3 to level 2 will generally be quite slow and can be neglected compared to competing processes (i.e., $Z_{32} \simeq 0$). This assumption will be valid for some atomic systems to be included in the experimental study to be reported later. For other systems which do not allow this assumption, experimental correction for thermally assisted population of level 3 could be made merely by monitoring emission from that level in the absence of exciting radiation (i.e., when $\rho_0 = 0$). If $Z_{32} = 0$, the rate of population of energy levels 2 and 3 [cf. Eqs. (24) and (25)] becomes:

$$\frac{dn_2(t)}{dt} = n_1 B_{12}\rho(t) - n_2(B_{21}\rho(t) + a_{23} + a_{21}) \tag{30}$$

and

$$\frac{dn_3(t)}{dt} = n_2 a_{23} + n_1 Z_{13} - n_3 a_{31} \tag{31}$$

To study the saturation of upper energy level 2, one must solve Eq. (30) as a function of time and incident power density. In turn, because the population of atoms free to absorb the exciting radiation (namely n_1) depends

partially upon the rate of population and depopulation of energy level 3, some considerations of level 3 are necessary to solve Eq. (30).

Thermal Equilibrium. First, consider the case where the energy difference between levels 3 and 1, $(E_3 - E_1)$ is comparable to or smaller than the thermal energy (kT) available from the flame environment. In this case, an equilibrium will exist between the population of levels 3 and 1 which can be described by the relation:

$$n_1 Z_{13} \approx n_3 a_{31} \tag{32}$$

Substitution of Eq. (32) into Eq. (29) yields the population of level 1:

$$n_1 = \frac{(N - n_2)}{(1 + Z)} \tag{33}$$

where

$$Z = Z_{13} / a_{31} \tag{34}$$

After substitution of Eq. (33) into Eq. (30), the rate of population of level 2 becomes:

$$\frac{dn_2(t)}{dt} = \frac{N\rho(t)B_{12}}{(1+Z)} - n_2 \left\{a_{21} + a_{23} + \rho(t) \left[B_{21} + \frac{B_{12}}{(1 + Z)}\right]\right\}$$

or

$$\frac{dn_2(t)}{dt} = c_{3e}\, \rho(t) - n_2(t) \left[a_{3e} + b_{3e}\, \rho(t)\right] \tag{35}$$

where the lumped parameters are defined as:

$$a_{3e} = a_{21} + a_{23} \tag{36}$$

$$b_{3e} = B_{21} + \frac{B_{12}}{(1 + Z)} \quad \text{and} \tag{37}$$

$$c_{3e} = \frac{NB_{12}}{(1 + Z)} \tag{38}$$

In these expressions, the subscripts 3 and e are used to indicate the three-level model and the assumption of equilibrium between energy levels 3 and 1.

A comparison of Eqs. (6) and (35) indicates that the same general expression for the rate of population of the upper level is obtained for a two-energy-level atomic system and a three-energy-level system, if in the latter model equilibrium is assumed between levels 3 and 1. Also, Eq. (35) reduces to Eq. (6) for the case $Z \tilde{<} 0$. In turn, Z would approach zero if energy level 3 had a negligible population compared to that of level 1 (cf. Eq. 34). This behavior would exist, for example, in the case of a very slow radiative population of level 3 from level 2, coupled with a much more rapid radiative depopulation of level 3. In such a situation, the dominant pathway for energy loss from level 2 would be the transition to level 1, (i.e., $A_{23} << A_{21}$). In such a case, one need consider only the $2 \rightarrow 1$ de-excitation path and can assume a two-energy level system.

Because of the similarity of Eqs (6) and (35), the same analysis which was performed for the two-level system on the population of the upper energy level could be applied to the present case of a three level system, with equilibrium between the two lowest energy levels (3 and 1).

Correspondingly, a saturation power density (ρ_{3es}) for direct-line fluorescence can be defined by reference to Eq. (11) as

$$\rho_{3es} = \frac{a_{3e}}{b_{3e}} \tag{39}$$

Steady-State Approximation. Another case worthwhile considering in direct-line fluorescence is that in which the rates of population and depopulation of level 3 are comparable, so that a steady-state population of that level is achieved. If

$$\frac{dn_3(t)}{dt} \tilde{=} 0,$$

the population of the lower energy level (n_1) can be found from Eq. (31):

$$n_1 = \frac{1}{(1 + Z)} \left\{ N - n_2(1 + a_{23}/a_{31}) \right\} \tag{40}$$

By substitution of Eq. (40) into Eq. (30), one obtains the following expression for the rate of population of level 2:

$$\frac{dn_2(t)}{dt} = \frac{NB_{12}\rho(t)}{(1+Z)} - n_2\left\{a_{21} + a_{23} + B_{21}\rho(t) + B_{12}\rho(t)\,\frac{(1+a_{23}/a_{31})}{(1+Z)}\right\}$$

or

$$\frac{dn_2(t)}{dt} = c_{3s}\,\rho(t) - n_2(t)\left[a_{3s} + b_{3s}\rho(t)\right] \tag{41}$$

where:

$$a_{3s} = a_{21} + a_{23} \tag{42}$$

$$b_{3s} = B_{21} + B_{12}\,\frac{(1 + a_{23}/a_{31})}{(1+Z)} \tag{43}$$

and

$$c_{3s} = \frac{NB_{12}}{(1+Z)} \tag{44}$$

As in the earlier case, the population of the excited level follows the same behavior as in the two-energy-level system, but with different a, b and c coefficients (cf. Eq. 6).

Stepwise Fluorescence

In atomic systems which exhibit stepwise fluorescence, the energy separation between excited energy levels 2 and 3 is often small enough that collisionally induced transitions from level 3 to level 2 (Z_{32}) cannot be neglected. However, the rates of collisional level-1-to-level-3 transitions become negligible because of the large energy spacing between those levels (corresponding to ultraviolet-visible frequencies). Under these conditions, $Z_{13} \approx 0$ and the rate of population of levels 2 and 3 are (from Eqs. (24) and (25):

$$\frac{dn_2(t)}{dt} = n_1 B_{12}\rho(t) - n_2\left[B_{21}\rho(t) + a_{23} + a_{21}\right] + n_3 Z_{32} \tag{45}$$

and

$$\frac{dn_3(t)}{dt} = n_2 a_{23} - n_3(a_{31} + Z_{32}) \tag{46}$$

Because the population of level 3 is determined solely by collisional and non-radiationally induced transitions, its population will vary as a direct function of that in level 2. Likewise, stepwise fluorescence detected as a transition from level 3 to level 1 will follow the same saturation behavior as the population of level 2.

To find a simple relationship expressing the population of level 2, it is necessary to make some simplifying assumptions. One such assumption is that of a steady-state population of level 3. If the rate of collisional deactivation of excited atoms from level 2 to level 3 is comparable to the radiational and collisional deactivations of level 3 to level 1, and from level 3 to level 2, one can assume a steady-state population of level 3 (i.e, $dn_3(t)/dt \approx 0$). In this case, the population of level 2 is:

$$\frac{dn_2(t)}{dt} = NB_{12}\rho(t) - n_2(t)\{b_{nr}\rho(t) + a_{nr}\} \tag{47}$$

where

$$b_{nr} = B_{21} + B_{12}\left[1 + \left(\frac{a_{23}}{a_{31} + Z_{32}}\right)\right] \tag{48}$$

and

$$a_{nr} = a_{21} + a_{23} - \frac{Z_{32}a_{23}}{a_{31} + Z_{32}} \tag{49}$$

As in the two cases treated earlier involving direct-line fluorescence, the population of excited level 2 follows the same qualitative dependence on the incident power density as did the upper level in a resonance transition. However, in the present case, the saturation power density is determined by

the rates of deactivation from level 2 to level 1 and from level 3 to level 1.

In other specific cases which involve stepwise fluorescence processes, it is possible to make different assumptions which can be used to simplify the form of Eq. (45). However, because stepwise fluorescence is not yet widely used in analytical atomic spectrometry, these cases were not individually treated.

CONCLUSIONS

The model for saturation of atomic levels presented in the preceding section is far more general than those ordinarily applied to saturated AFS (1-10, 18, 19). Not only does the model lend itself to the convenient description of saturation effects in non-resonance fluorescence, it also is applicable to atomic systems driven toward saturation by transient pulses.

With this theoretical treatment, it becomes possible to predict the effect of various experimental variables on the saturation process. As an example, Figure 8 displays the predicted dependence of saturation spectral power density (ρ_s) on the duration (t_0) of the exciting radiation pulse. The case shown is the Ba transition at 553.5 nm, with an assumed lifetime (τ) of 8.5 ns and a collisional quenching rate equal to $10A_{21}$. Consequently, the true excited state lifetime ($\tau' = 1/(A_{21} + Z_{21})$) is approximately 0.8 ns. One can see from Figure 8 that the saturation spectral power density increases markedly as the excitation pulse becomes narrower than the true lifetime, but becomes nearly constant for excitation pulses much longer than the lifetime.

No attempt has been made to exhaustively illustrate the applicability of the model to non-resonance AFS. Rather, the two most commonly employed non-resonance methods (direct-line and stepwise fluorescence) were selected to show how pertinent excited-state populations could be predicted and how these populations relate to exciting source powers necessary to reach saturation.

The calculation of source power densities necessary to produce saturation is perhaps the most significant capability of the proposed model. With such a capability, it should be possible to predict the spectral power density which would generate saturation effects of the kind found to be so beneficial to analytical AFS. As we hope to show in a later communication,

accurate measurement of these required spectral power densities is extremely tedious and must be performed with great care. With knowledge of these requisite power levels, it should be possible to assess the feasibility of approaching atomic saturation with conventional (non-laser sources.

As with all theoretical models, the one proposed herein must be supported by experimental evidence. A study to provide this evidence has already been completed and will be reported shortly. In that study, the proposed model has been found to agree far better than earlier models with experimental results and can be used to determine values and trends relating to the saturation of atomic energy levels.

GLOSSARY

$a_2 = A_{21} + Z_{21} = 1/\tau'$ for 2-level atomic model

$b_2 = B_{12} + B_{21}$ for 2-level atomic model

a_{3e}, b_{3e}, c_{3e} = lumped parameters referring to 3-energy level model with the assumption of thermal equilibrium between levels 3 and 1. See Eqs. 36-38.

a_{3s}, b_{3s}, c_{3s} = lumped parameters pertaining to direct-line fluorescence from a 3-level atomic model in which the lower level involved in the transition is assumed to have a steady-state population. See. Eqs. 42-44.

a_{nr}, b_{nr} = lumped parameters pertaining to stepwise fluorescence from a 3-level atomic model in which a steady-state population is assumed for the upper level in the fluorescence transition. See. Eqs. 48-49.

A_{ji} = Einstein coefficient for spontaneous emission from level j to level i (sec^{-1})

B_F = detected fluorescence radiance

c = speed of light (3×10^{10}cm/sec)

D = departure of rate-controlled average population of excited level (under non-steady-state irradiation) from the population produced by steady-state irradiation. See Eq. 18.

E_i = Energy of atomic level i

ε = Fractional (as %) error in saturation spectral power density caused by erroneous assumption of steady-state irradiation.

g_i = degeneracy (statistical weight) of the ith energy level

h = Planck's constant = 6.624×10^{-34} J-sec

k = Boltzmann constant

λ_{ji} = wavelength corresponding to a transition from energy level j to energy level i

$n_i(t)$ = Number of atoms in energy level i at time t

N = total number of atoms in all levels under consideration

N_2^{SS} = Steady-state population of upper level 2 produced by continuous irradiation

$N_j = \overline{n_j(t)}$ = average number of atoms in upper level j during the excitation pulse

$(N_j)_{sat}$ = population of level j under conditions of complete saturation.

ν_{ji} = spectral frequency corresponding to a transition from level j to level i

ρ_{3es} = saturation spectral power density corresponding to direct-line fluorescence from a 3-energy level model atom with assumed thermal equilibrium between levels 1 and 3

$\rho(t)$ = spectral power density of incident beam (watts/cm^{2}Hz)

ρ_0 = peak spectral power density of exciting radiation

$\rho_s = \frac{a_2}{b_2}$ = saturation spectral power density for 2-level atomic model

ρ_s^{NSS} = peak spectral power density of a transient (non-steady-state) excitation pulse which produces an excited level population half that generated during saturation. Termed the non-steady-state saturation spectral power density.

t = time

t_0 = excitation pulse length.

T = absolute temperature (°K)

τ' = observed fluorescence lifetime for transition of interest = $1/a_2$

$Z = Z_{13}/a_{31}$ (see Eq. 34)

Z_{ij} = rate of collisional (radiationless) transition from level i to level j (sec^{-1})

Z_{21}/A_{21} = quenching factor for a 2-level model

REFERENCES

1. Denton, M.B. and Malmstadt, H.V., Appl. Phys. Lett. 18, 485 (1971).

2. Fraser, L.M. and Winefordner, J.D., Anal. Chem. 43, 1693 (1971).

3. Kuhl, J., Marowsky, G. and Torge, R., Anal. Chem. 44, 375 (1972).

4. Omenetto, N., Hatch, N.N., Fraser, L.M. and Winefordner, J.D., Anal. Chem. 45, 195 (1973).

5. Kuhl, J. and Spitschan, H., Opt. Comm. 7, 256 (1973).

6. Kuhl, J., Neumann, S. and Kriese, M., Z. Naturforsch 28A, 273 (1973).

7. Neumann, S. and Kriese, M., Spectrochim. Acta 29B, 127 (1974).

8. Fraser, L.M. and Winefordner, J.D., Anal. Chem. 44, 1444 (1972).

9. Omenetto, N., Hatch, N.N., Fraser, L.M. and Winefordner, J.D., Spectrochim. Acta 28B, 65 (1973).

10. Omenetto, N., Hart, L.P., Benetti, P. and Winefordner, J.D., Spectrochim. Acta 28B, 301 (1973).

11. Piepmeier, E.H., Spectrochim. Acta 27B, 431 (1972).

12. Piepmeier, E.H., Spectrochim. Acta 27B, 445 (1972).

13. Omenetto, N., Benetti, P., Hart, L., Winefordner, J.D. and Alkemade, C. Th. J., Spectrochim. Acta 28B, 289 (1973).

14. Omenetto, N. and Winefordner, J.D., Appl. Spectrosc. 26, 555 (1972).

15. Schenck, P., Hilborn, R.C. and Metcalf, H., Phys. Rev. Lett. 31, 189 (1973).

16. Mitchell, A.C.G. and Zemanski, M.W., "Resonance Radiation and Excited Atoms", Cambridge Press, Cambridge (1961).

17. Kelly, F.M., Koh, T.K. and Mathur, M.S., Can. J. Phys. 52, 795 (1974).

18. Omenetto, N., Winefordner, J.D., and Alkemade, C. Th.J., Spectrochim. Acta 30B, 335 (1975).

19. Brod, H.L. and Yeung, E.S., Anal. Chem. 48, 344 (1976).

CREDIT

Supported in part by the National Science Foundation through grant MPS-75-21695 and by the Office of Naval Research.

ACKNOWLEDGEMENT

The authors would like to thank Nicolo Omenetto for his useful comments and suggestions during the early stages of this investigation.

Table I. Saturation power density as a function of the duration of the excitation pulse for the $S_0 \rightarrow P_1$ transition of Ba (553.5 nm)

t_o (nsec)	ρ_o (watts/cm^2 Hz) x 10^{+9}
1	1.31
10	0.70
1000	0.65

Table II. Saturation Spectral Power Densities (ρ_s) predicted by Eq. (17) for atoms experiencing various rates of collisional quenching (Z_{21}) and being excited by different pulse lengths.

Z_{21}/A_{21}	$\rho_s[(W/cm^2 \cdot Hz) \times 10^9]$ for excitation pulse length of 1 μs	$\rho_s[(W/cm^2 \cdot Hz) \times 10^9]$ for excitation pulse length of 6.5 ns	ε Relative Error Generated by Assuming Steady-State Irradiation of Atoms (%)
0	0.06	0.16	62
5	0.35	0.44	20
10	0.64	0.73	12

Table III. Dependence of calculated saturation spectral power density on the assumed value of the fluorescence lifetime

Assumed Lifetime of Atomic Transition τ (ns)	ρ_s (W/cm^2 Hz) x10^9	ε^a(%)
4	.64	} 11
8	.72	
16	1.0	} 30

a. The parameter ε expresses the per cent error in the predicted saturation power density which would be caused by assuming a value for the fluorescence lifetime (τ) that is 50% in error.

Table IV Values of saturation power density predicted by the two energy-level model

Element	Transition	λ(nm)	τ(s)	(Ref.)	ρ_s (W/cm² Hz) x 10^9
Mg	$^1S_0 \rightarrow {}^1P_1$	285.2	3.3×10^{-9}	(16)	4.9
Cd	$^1S_0 \rightarrow {}^3P_1$	326.1	3.5×10^{-6}	(16)	250.
Ca	$^1S_0 \rightarrow {}^1P_1$	422.7	4.6×10^{-9}	(15)	1.5
In	$^2P_{\frac{3}{2}} \rightarrow {}^2S_{\frac{1}{2}}$	451.1	9.0×10^{-9}	(16)	3.5
Sr	$^1S_0 \rightarrow {}^1P_1$	460.7	4.7×10^{-9}	(17)	1.8
Tl	$^2P_{\frac{3}{2}} \rightarrow {}^2S_{\frac{1}{2}}$	535.0	9.0×10^{-9}	(16)	2.1
Li	$^2S_{\frac{1}{2}} \rightarrow {}^2P_{\frac{1}{2}}$	670.8	27.0×10^{-9}	(16)	1.0

Figure 1. Schematic diagram for excitation and saturation of a two energy level atomic system.

A) Energy level diagram showing transition rates; B_{12} and B_{21} are the Einstein coefficients for induced transitions ($1 \rightarrow 2$ and $2 \rightarrow 1$) respectively, A_{21} is the Einstein coefficient for spontaneous emission ($2 \rightarrow 1$), Z_{21} is the rate for the collisionally induced transition ($2 \rightarrow 1$) and $\rho(t)$ is the spectral power density of the exciting beam of radiation, $a_2 = A_{21} + Z_{21}$

B) Boxcar function assumed to describe the time behavior of the exciting radiation; t_0 and ρ_0 are the width and the peak spectral power density of the radiation pulse, respectively.

Figure 2. Time behavior of the fraction of excited atoms (solid curve) during application of a 5 ns duration pulse of exciting radiation. Pertinent assumed rate constants governing excitation and decay are given in the text.

$\frac{N_2}{N}$ = fractional population of excited state. Rise and fall times calculated at 1/e points.

Figure 3. Fraction of excited atoms produced by non-steady state irradiation by a laser of varying spectral power density. Degrees of excitation for various pulse lengths (t_0) are shown.

A) t_0 = 1 μs
B) t_0 = 10 ns
C) t_0 = 1 ns

Fraction of atoms in excited state when laser power density is infinite = 0.75 (see text for explanation).

Figure 4. Predicted saturation curves showing the effect of quenching collisions on excited-state population. Excitation pulse is of 1 μs duration. Curves A, B and C correspond to atom environments in which the rates of collisions are 0, 5 and 10 times the rate of spontaneous emission, respectively. N_2/N is the fraction of all atoms in the upper state; for complete saturation, N_2/N = 0.75.

Figure 5. Predicted saturation curves showing the effect of quenching collisions on excited-state population. Excitation pulse of 6.5 ns duration. Curves A, B, and C correspond to atom-environments in which the rates of collisions are 0, 5 and 10 times the rate of spontaneous emission, respectively. Compare to Figure 4.

Figure 6. Effect of the accuracy of the values of fluorescence lifetime on the saturation curves.

A) τ = 4 ns
B) τ = 8 ns
C) τ = 16 ns

Figure 7. Schematic model for excitation and saturation of a three-energy level atomic system.

A) Energy level diagram showing the activation and deactivation pathways.

B) Boxcar function assumed to describe the time behavior of the exciting radiation.

See text for discussion of rates of various transitions.

Figure 8. The predicted effect of excitation pulse length on saturation spectral power density for the Ba 553.5 nm transition. True lifetime of the transition assumed to be 0.8 ns.

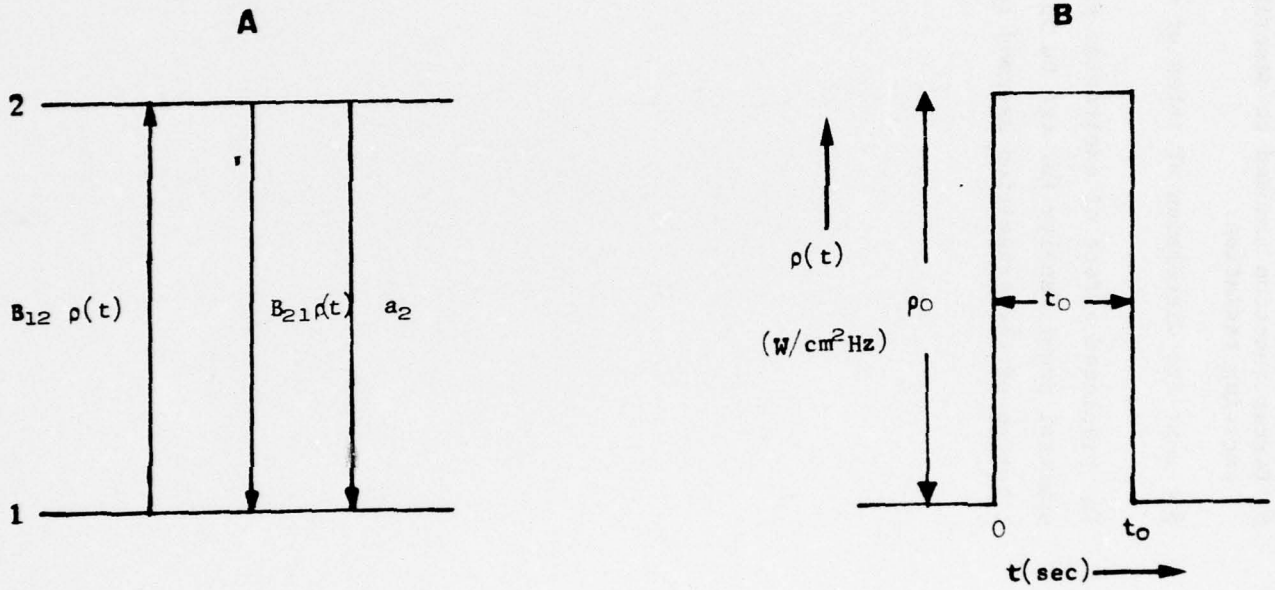
A
2
1
$B_{12}\ \rho(t)$
$B_{21}\rho(t)$
a_2
B
$\rho(t)$
(W/cm^2Hz)
ρ_o
t_o
0
t_o
t(sec)

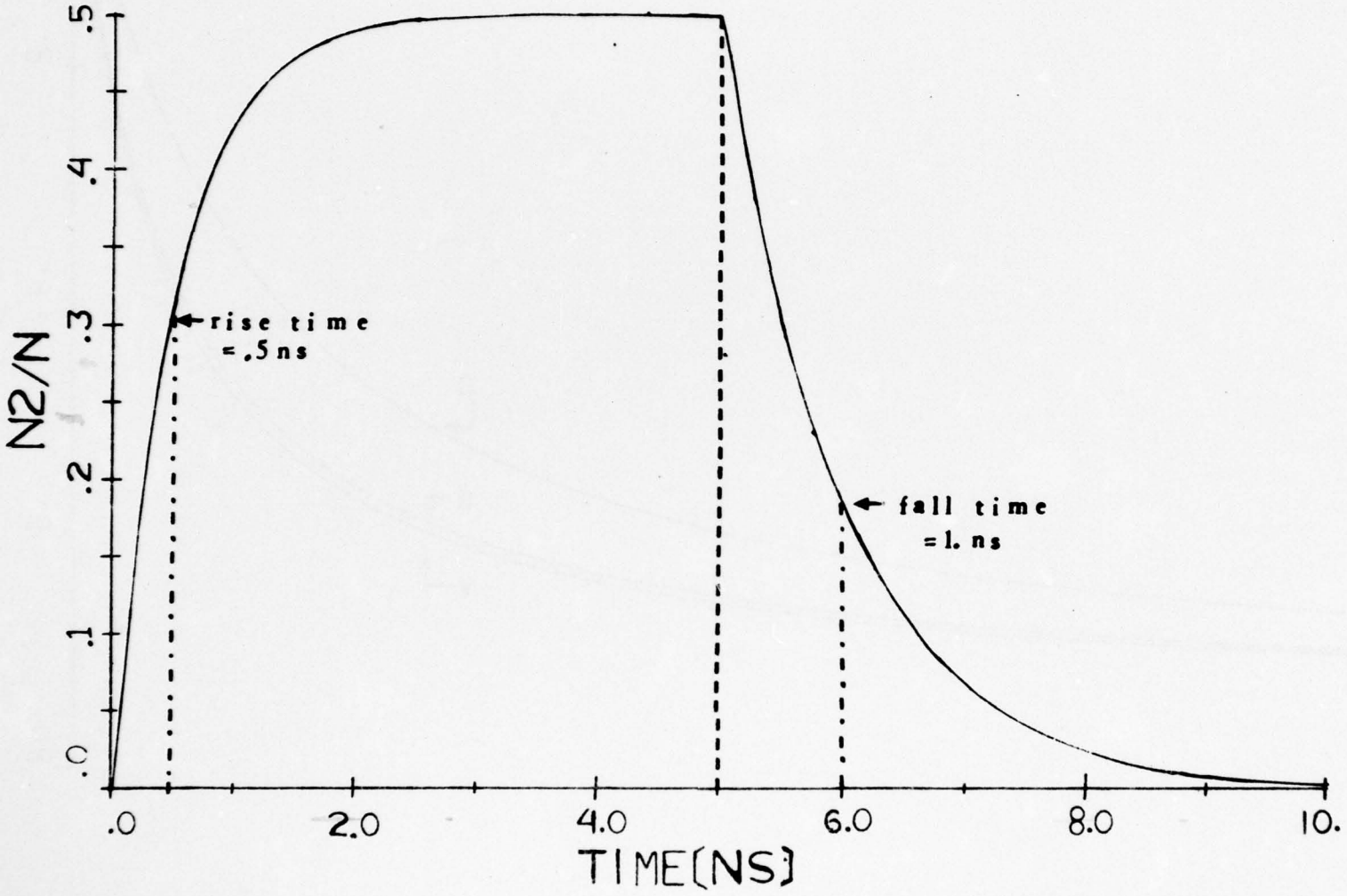
N2/N
.0
.1
.2
.3
.4
.5
rise time
=.5ns
fall time
=1. ns
.0
2.0
4.0
6.0
8.0
10.
TIME(NS)

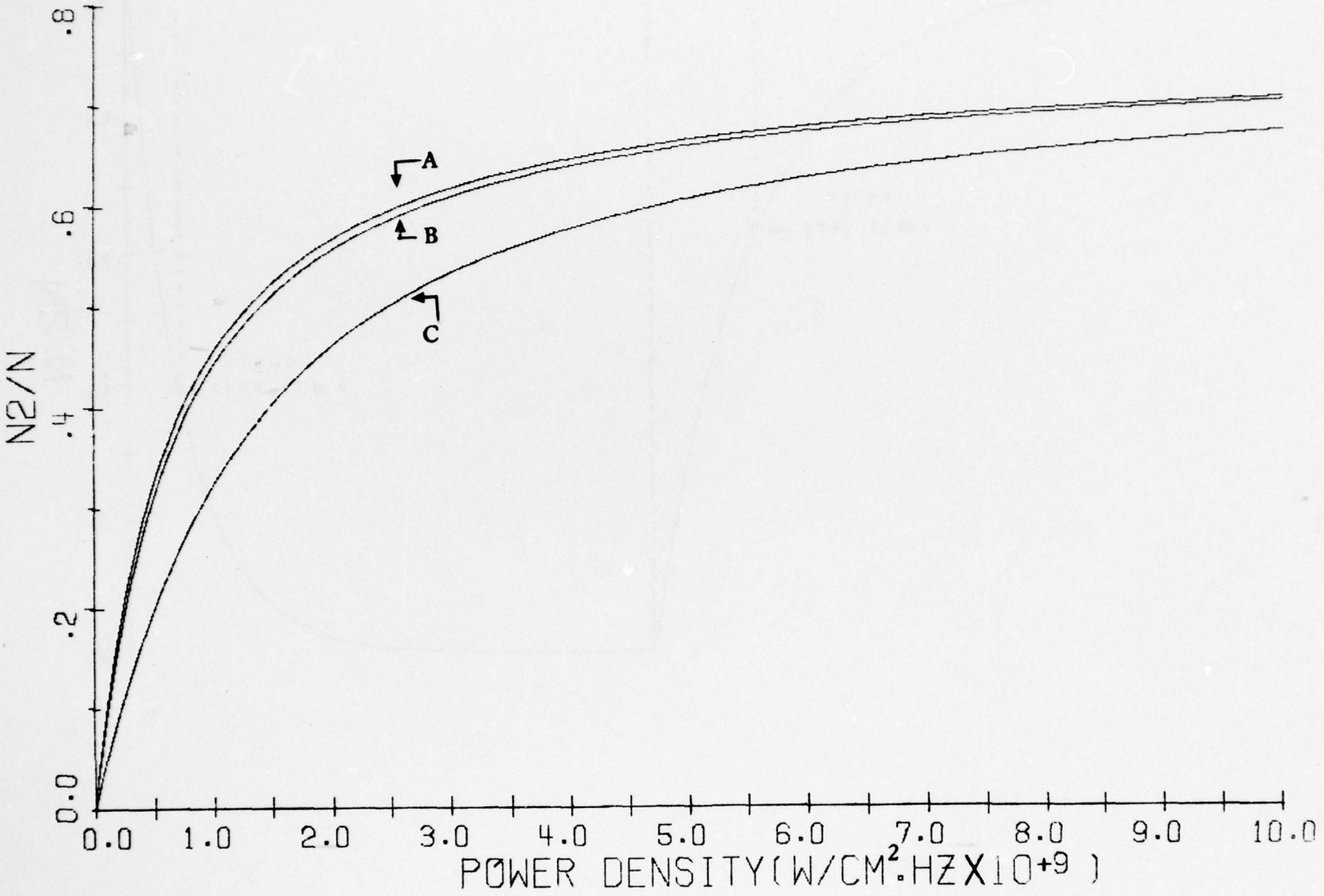
N2/N
0.0
.2
.4
.6
.8
A
B
C
0.0
1.0
2.0
3.0
4.0
5.0
6.0
7.0
8.0
9.0
10.0
POWER DENSITY(W/CM².HZX10+9)

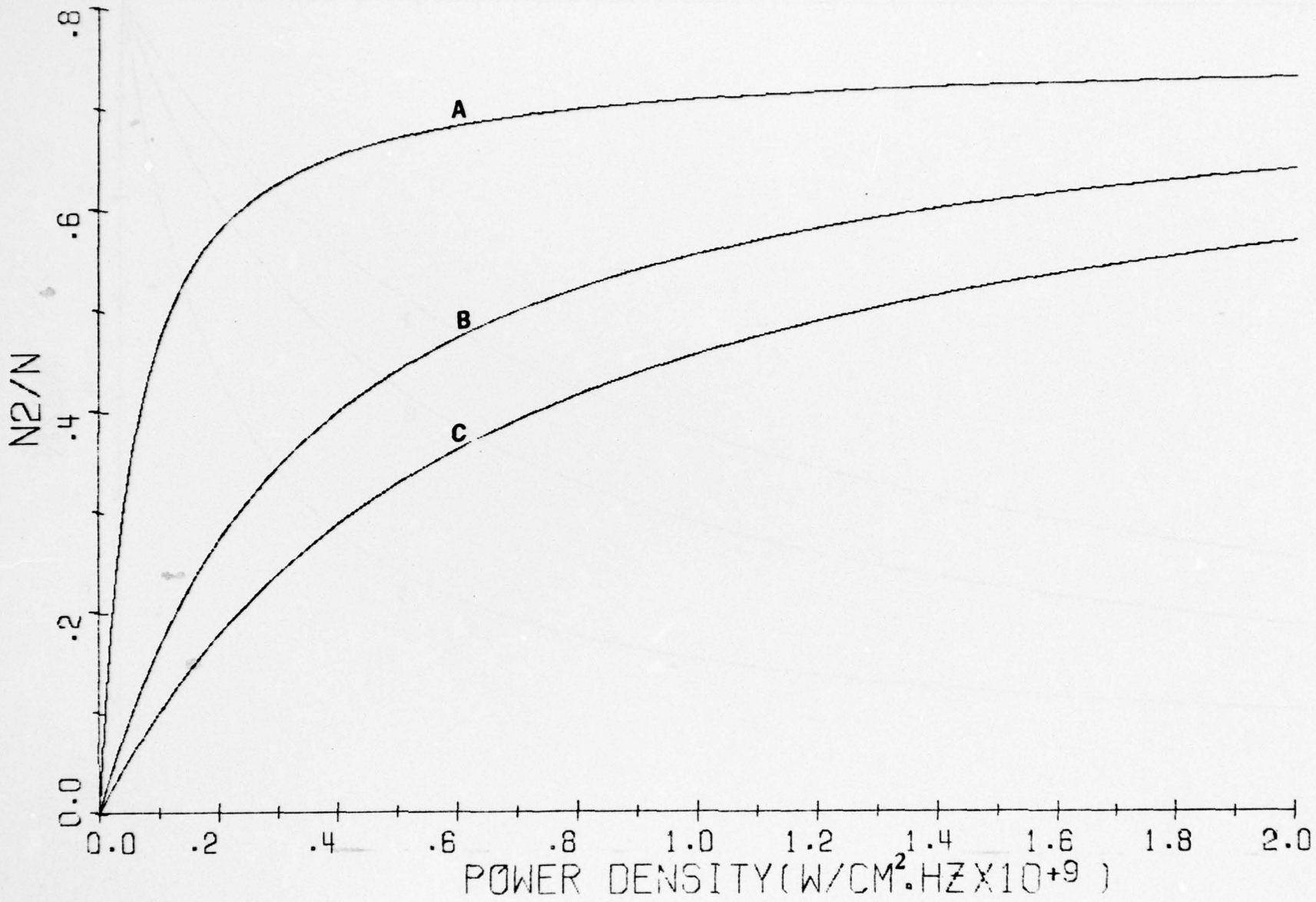
N2/N
0.0
.2
.4
.6
.8
A
B
C
0.0
.2
.4
.6
.8
1.0
1.2
1.4
1.6
1.8
2.0
POWER DENSITY(W/CM².HZX10+9)

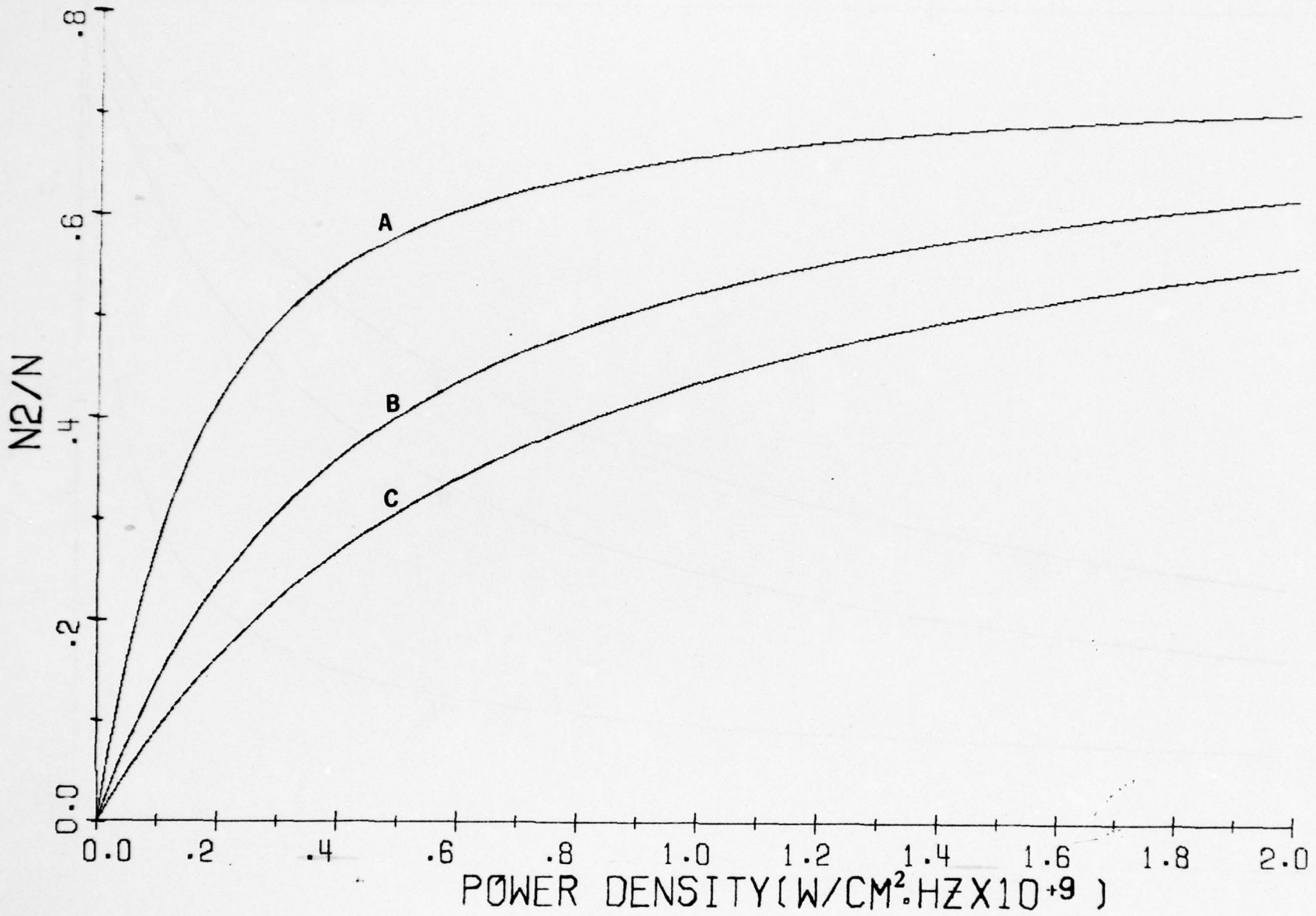
N2/N
0.0
.2
.4
.6
.8
A
B
C
0.0
.2
.4
.6
.8
1.0
1.2
1.4
1.6
1.8
2.0
POWER DENSITY(W/CM².HZX10+9)

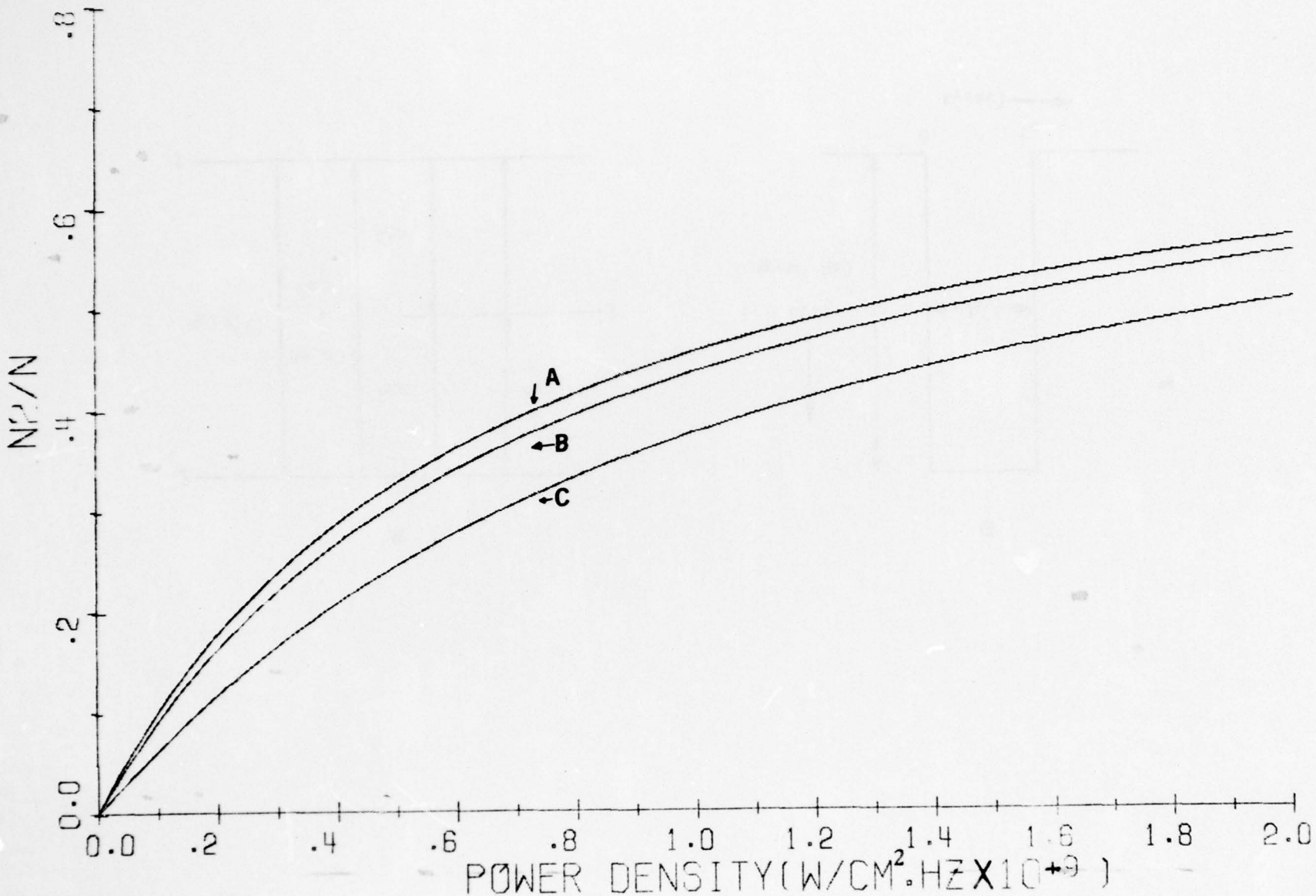
NP/N
0.0
.2
.4
.6
.8
A
B
C
0.0
.2
.4
.6
.8
1.0
1.2
1.4
1.6
1.8
2.0
POWER DENSITY(W/CM².HZ X10⁺⁹)

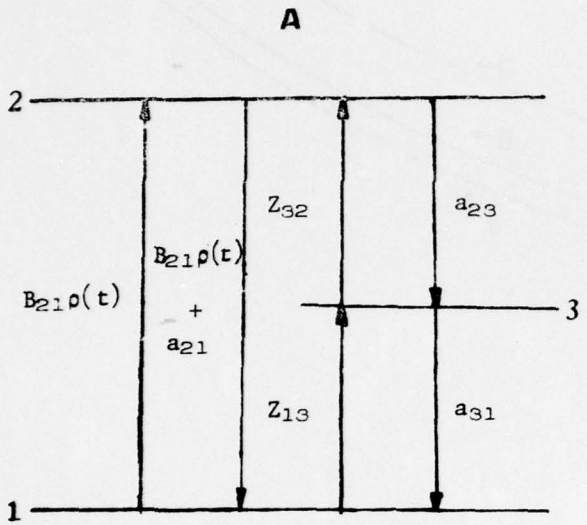
A
2
1
3
Z_{32}
a_{23}
$B_{21}\rho(t)$
$B_{21}\rho(t)$
+
a_{21}
Z_{13}
a_{31}

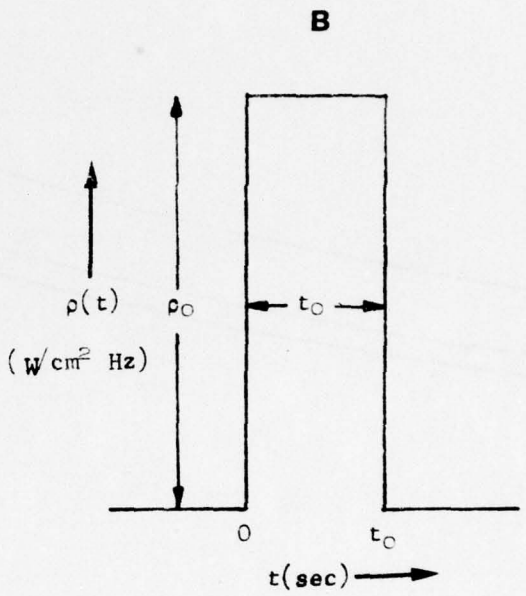
B
$\rho(t)$
$(W/cm^2\ Hz)$
ρ_o
t_o
0
t_o
t(sec)

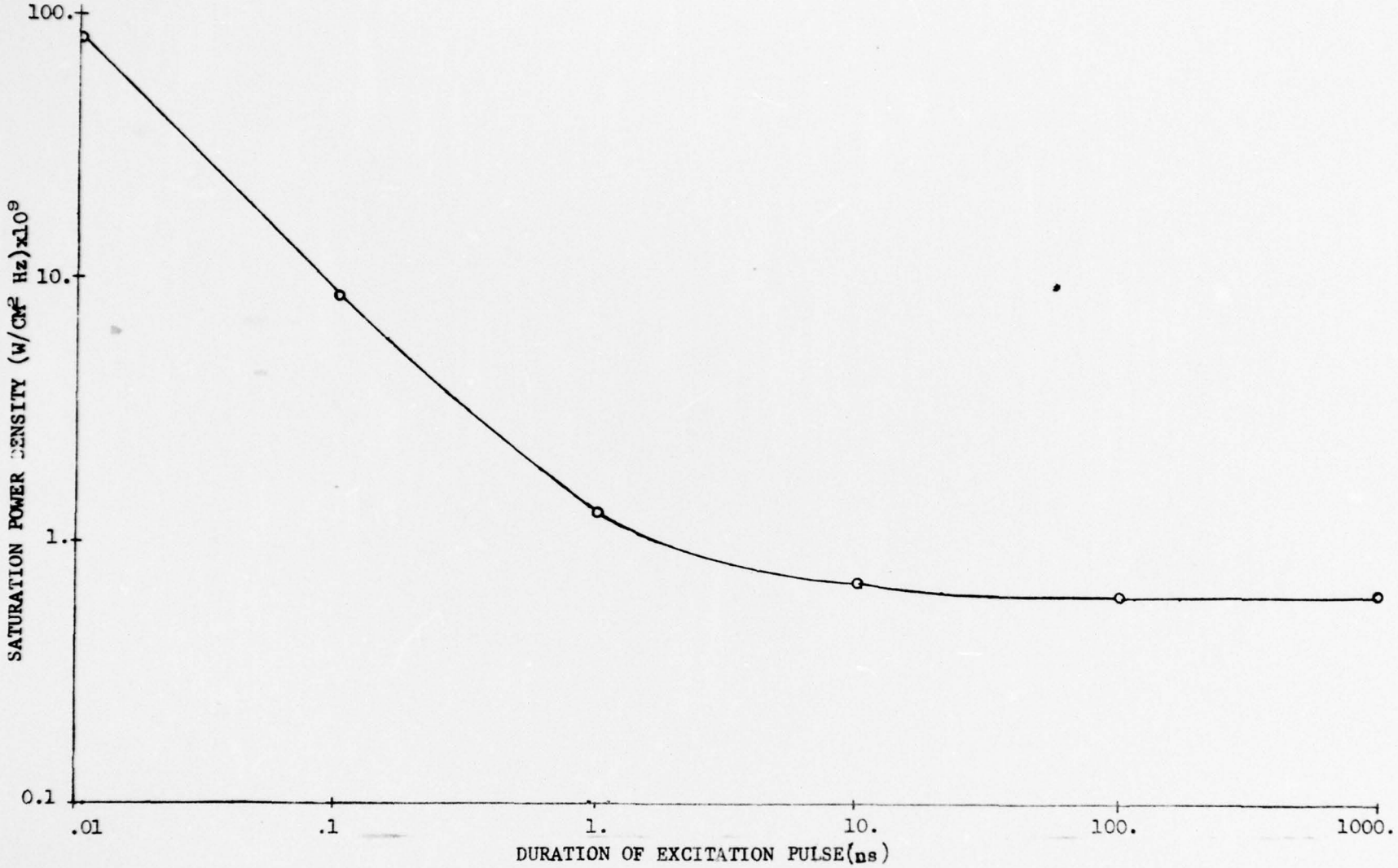
100.
10.
1.
0.1
SATURATION POWER DENSITY (W/CM² Hz)x10⁹
.01
.1
1.
10.
100.
1000.
DURATION OF EXCITATION PULSE(ns)